INVESTIGATIONS INTO THE NOISE CHARACTERISTICS OF DIGITIZED AERIAL IMAGES

Barbara Waegli
Institut für Photogrammetrie, Universität Bonn
Nußallee 15, D-53115 Bonn

Commission II, Working Group 8 (Proceedings ISPRS Comm. II Symposium, Cambridge, UK, 13-17 July 1998)

KEY WORDS: noise variance, robust variance estimation, scanner characteristics, digitized transparencies

ABSTRACT

For automated image evaluation a precise characterization of the noise behaviour of the image data is needed. Digital image acquisition in aerial photogrammetry usually is performed by digitizing analogue film material. The noise of the digital image is composed of the noise due to the digitization process and of the noise of the analogue image. From a statistical point of view, noise can be described by the standard deviation and the correlation of the fluctuation of the intensity values. Our aim is to determine a noise model out of the images itself, without the need of special test patterns. We do this by following two approaches: pixelwise evaluation of multiple scans of the film material and regionwise evaluation from a single scan. The first approach analyses the noise coming from the digitization process, while in the second case we obtain the complete noise budget. We analyze the correlation between successive scans. First empirical investigations with different film material were performed and the results are presented.

1 INTRODUCTION

Whenever processing digitized aerial images, we have to deal with noise, coming from the film and the scanner used for the digitization. The results of image processing depend on the quality of the input data. For automated image evaluation a precise characterization of the noise behaviour is needed. The image model should be generic enough to permit the determination of the model parameters out of the image itself, without the need of a separate calibration or special test patterns, and with no additional information about the film or the scanner. This paper is addressed to the problem of automatic noise estimation for the use in image processing.

Aerial images currently are and in the foreseeable future still will be recorded with film-based systems and digitized later to enable a digital processing. Therefore the noise effects present in analogue images and the ones caused by the digitization process have to be considered.

The noise characterization of analogue photographs has been object of different contributions in the past (e.g. by [Dainty and Shaw, 1974, Diehl, 1990, Diehl, 1992]). [Lenz, 1988] analyzed the case of CCD cameras, i.e. directly digitally recorded images. In [Brügelmann and Förstner, 1992] a robust procedure for the estimation of the signal dependent components of the noise variance is given. They assume image noise variance to be either constant or linear dependent on the signal intensity, a model which is adequate for CCD-Cameras. During the last years various publications on the analysis of film scanners appeared (e.g. [Bolte et al., 1996, Baltsavias et al., 1997, Baltsavias and Käser, 1998, Häring et al., 1998]), where the noise behaviour is usually determined by means of the variance of homogeneous regions (usually the different density steps of a grey level wedge).

In this contribution we make no assumption about the form of the functional connection between the noise variance and the signal intensity, as the determination of the noise variance function is our goal. We use the digital image itself instead of special test patterns (e.g. a grey level wedge). Our investigations are restricted to greyscale images, however the methodology can easily be transferred to multiband images.

In the following we will determine the noise variance function for images of different type, to be able to ascertain which shared characteristics possibly lead to a common model. The final aim is a noise model which can be implemented as a preanalysis step in image processing procedures without the need of any additional parameters.

2 NOISE IN DIGITIZED IMAGES

Noise is a stochastic disturbance superimposed onto the signal. It has to be distinguished from texture, e.g. in images of vegetation. It causes an uncertainty of the greyvalue in the scanned image for a certain position in the image. Noise can be described by the standard deviation and the correlation of the fluctuation of the greyvalues.

The measured intensity function $g(i,j)$, depending from the position (i,j) can be written as a superposition of the true signal $f(i,j)$ and the noise $n(i,j)$:

$$g(i,j) = f(i,j) + n(i,j) \tag{1}$$

During every stage from the image acquisition to the digitized image new noise components join the noise budget. If the image acquisition takes place with a film camera, we have to take into account the film graininess. Digital camera as well as image scanners work with a CCD sensor, where noise is caused by the CCD, the CCD readout-electronic, the A/D-converter. Another noise source in an image scanner is the illumination source. During image recording, film development and digitization dust can affect the image quality.

Therefore we can distinguish several noise categories, divided by its sources:

- atmospheric noise σ_a
- the film granularity σ_f
- photoelectronic noise σ_p
- electronic noise σ_e
- quantization noise σ_q

The total noise variance σ_n can be obtained summing up the single components:

$$\sigma_n^2 = \sigma_a^2 + \sigma_f^2 + \sigma_p^2 + \sigma_e^2 + \sigma_q^2 \tag{2}$$

The noise components can be randomly distributed (e.g. dust) or constant (i.e. signal independent) or signal dependent (e.g the photoelectronic noise, or the distribution of the silver halide crystals in the film).

In the digitized image they are all superimposed, so that the effect of the single stages cannot be easily separated.

The noise variance σ_n is supposed to be dependent of the intensities $g(i,j)$:

$$\sigma_n^2 = \phi\big(g(i,j)\big) \tag{3}$$

The noise variance is assumed to be independent of the position, given by i and j.

The dependency itself, however, is unknown. Though in general we have to assume the noise of neighbouring pixels to be correlated, we do not analyse this dependency here.

Positive images are expected to show higher noise in bright parts, while if we get the positive digital image by scanning a negative, we will have higher noise in the darker parts of the image.

There are two possibilities to eliminate the effects of noise:

a. noise reduction (e.g. by filtering): this leads to a reduction of noise, but the quality of the image information (features and discontinuities) is also affected to some extent.

b. noise estimation and consideration: in this case a model for the noise has to be formulated and taken into account, e.g. when choosing thresholds.

In both cases we need to know the specific characteristics of the image noise.

3 THEORETICAL BASIS FOR ESTIMATING NOISE CHARACTERISTICS

To build a noise variance model for digitized images we follow two approaches: the determination of the noise variance of the scanner by means of *multiple* scanned images, and the determination of the whole noise budget out of a *single* scan.

3.1 Noise variance estimates from multiple scans

When using multiple scans of an image, it is possible to determinate the variance of the intensity for every single pixel. The determined noise variance corresponds to the noise rate due to the scanning device, while the other noise components are eliminated:

$$\sigma_n^2 = \sigma_p^2 + \sigma_e^2 + \sigma_q^2 \tag{4}$$

We compute the mean

$$\overline{g}(i,j) = \frac{1}{N}\sum_{k=1}^{N} g_k(i,j) \tag{5}$$

N= number of images, g= intensity

and the estimated variance

$$\widehat{\sigma}^2_{n,mean}\big(g(i,j)\big) = \frac{1}{N-1}\sum_{k=1}^{N}\big(g_k(i,j) - \overline{g}(i,j)\big)^2 \tag{6}$$

To get a robust estimation for the noise variance, we compute the median

$$\mathrm{med}\big(g(i,j)\big) = g_{p=\frac{1}{2}}(i,j) \tag{7}$$

and the median absolute deviation (MAD)

$$\mathrm{MAD}(g) = \mathrm{med}\big|g_k - \mathrm{med}(g)\big| \tag{8}$$

over the multiple scans for each pixel.
By means of the positive median absolute deviation (MAD^+)

$$\mathrm{MAD}^+(g) = \mathrm{med}\big|g_k - \mathrm{med}(g)\big| \quad \big(g_k - \mathrm{med}(g)\big) > 0 \tag{9}$$

and the negative median absolute deviation (MAD^-)

$$\mathrm{MAD}^-(g) = \mathrm{med}\big|g_k - \mathrm{med}(g)\big| \quad \big(g_k - \mathrm{med}(g)\big) < 0 \tag{10}$$

the behaviour in the positive and negative neighbourhood of the median can be observed separately.

A robust estimate for the standard deviation $\widehat{\sigma}_n$ can be written as follows:

$$\widehat{\sigma}_{n,med} = c{\cdot}\mathrm{MAD} \quad , \quad c = \frac{1}{\Phi^{-1}(0.75)} \approx \frac{1}{0.78} \tag{11}$$

and will be used to evaluate the positive and negative part of the standard deviation $\sigma_{n,med+}$ and $\sigma_{n,med-}$.

3.2 Correlation between successive scans

The main assumption on which the analysis of multiple scans is based is the repeatability of a scan. The reliability of this assumption can be checked by computing the correlation function

$$\rho_{g'g''}(u,v) = \frac{\sum_{ij}\big(g'(i,j) - \overline{g'}\big){\cdot}\big(g''(i-u,j-v) - \overline{g''}\big)}{\sqrt{\sum_{ij}\big(g'(i,j) - \overline{g'}\big)^2 {\cdot} \sum_{ij}\big(g''(i,j) - \overline{g''}\big)^2}} \tag{12}$$

between the images of one scan sequence. In the ideal case in which the repeated scans are identical, the maximal correlation would be found for $u = v = 0$ and $\rho(0,0) = 1$. $\rho_{g'g''} \doteq \rho_{g'g''}(0,0)$ is called the correlation coefficient between the functions g' and g''.

The average noise variance can also be estimated by means of the signal-to-noise ratio (SNR)

$$SNR = \frac{\sigma_f}{\sigma_n} = \sqrt{\frac{\rho}{1-\rho}} \tag{13}$$

where σ_f is the signal standard deviation, σ_n the noise standard deviation and ρ the correlation coefficient between two images having the same noise and signal characteristics. This, compared to equation (3), simplified relation assumes the noise variance to be signal independent.

By solving equation (13) we obtain an average value

$$\sigma_n = \sigma_f \sqrt{\frac{1-\rho}{\rho}} \tag{14}$$

from the signal standard deviation and a correlation coefficient.

3.3 Noise variance from single scans

For the determination of the intensity variance out of a single image we use homogeneous regions in the digitized image. A homogeneity measure, e. g. the gradient magnitude, allows the exclusion of regions with rough intensity surfaces or very irregular texture, which would lead to a falsification of the results.

The variance obtained this way contains, beside the noise components mentioned above, the influence of moderate texture which cannot be caught by thresholding the homogeneity measure, representable by σ_t:

$$\sigma_n^2 = \sigma_a^2 + \sigma_f^2 + \sigma_p^2 + \sigma_e^2 + \sigma_q^2 + \sigma_t^2 \qquad (15)$$

We determine the intensity variances over homogeneous regions using equation (6). Homogeneous regions are connected components where the local gradient is non significant. Therefore smooth variations within a region are allowed and will significantly increase the estimate value for σ_n. In case the aim is to determine the behaviour of the noise variance for the entire intensity range (from 0 to 255), test clippings with a large number of homogeneous regions covering a large intensity range are needed.

4 EMPIRICAL INVESTIGATIONS

4.1 Test material

For the investigation, we scanned different aerial images:

- b/w film, negative, original
- b/w film, positive, copy from negative original
- color film, positive

As the exact film type used for the test images is unknown, we can just refer to it in the terms above.

All images were digitized as greyscale images. The scan parameters were optimized for each image. The scan resolution was chosen to be 14 μm, as this resolution is often used to digitize aerial images. Every image was scanned 10 times within a short time interval.

The test images were scanned with a Zeiss SCAI film scanner and the scan software PHODIS SC (cf. [Roth, 1996, Baltsavias and Käser, 1998]). The scanner is a flatbed scanner with stationary stage and moving sensor, optics and illumination. The sensor is a trilinear colour CCD Thomson THX7821 CCC with 8640 elements, out of which only the central 5632 are used. The geometric accuracy (standard deviation, according to [Baltsavias and Käser, 1998]) is better than 2 μm. The optical resolution of the scanner amounts to 7 μm, and it is possible to scan with pixel sizes of 7 μm,14 μm,21 μm,28 μm,56 μm,112 μm and 224 μm. The generation of the different pixel sizes is achieved in the scan direction by increasing the scan speed and in the CCD line by pixel averaging (for pixel sizes >7 μm). The scan is performed with 12 bit and stored with 8 bit. The scan parameters are defined through the minimum and maximum density over a region-of-interest (ROI) given by the user. They are automatically determined by the software using the prescan image and the histogram information. Color corrections are also possible.

For the analysis one or more clippings sized 300×300 [pel] or 500×500 [pel] were cropped from the scanned image (cf. Figure 1, Table 1). A smaller clipping C' (of 100 × 100 [pel]) lying inside clipping C was used mainly for the analysis of the correlation between the scans of one image series. Regarding the intensity distribution, which was optimal for the whole image, the situation is different for the single clipping, representing only a small part of the whole. In Figure 1 we can recognize saturated regions (clippings A2, B), regions with low contrast, clippings with only a small intensity range (clipping C, D3).

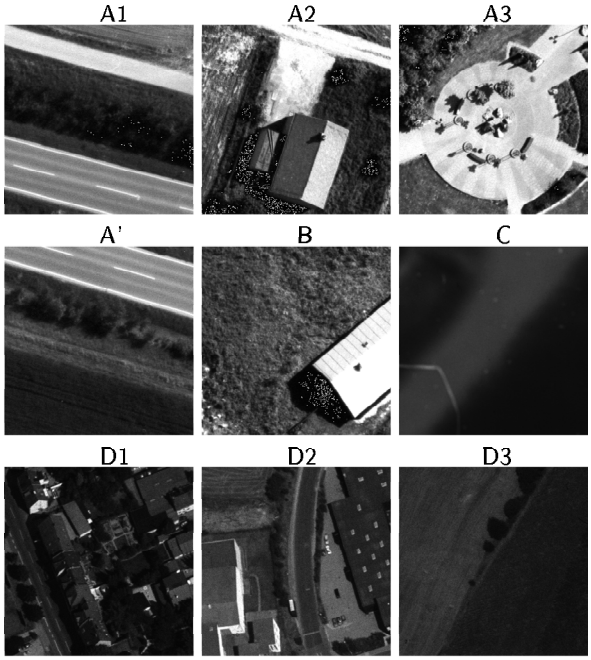

Figure 1: Test clippings (description of the images cf. Table 1)

name	size [pel]	film characteristics
A1	300×300	
A2	300×300	b/w negative
A3	300×300	
A'	300×300	same image as A, scanned at a different time
B	300×300	b/w negative
C	500×500	b/w positive copy from negative original
C'	100×100	is part of C
D1	500×500	
D2	500×500	color positive
D3	500×500	

Table 1: Image denomination and characteristics

4.2 Noise variance from multiple scans

To analyse the form of the noise variance function, we approximate it by building classes covering 8 greyvalues. Classes containing the realizations of one single greyvalue give information about the detailed behaviour of the function. The noise standard deviation value assigned to one class corresponds to the median of the root mean square of the variance values computed for the single pixels.

In the second and the third row of diagrams in Figure 3, the behaviour of $\sigma_{n,mean}(g)$ is plotted as a function of the intensity g for the image clippings B, A3 and D2.

The curves reveal several local maxima. At these maxima the scatter of the estimated variances is larger than in the neighbourhood. This applies to all the test clippings. We even could not find a relation between the curves belonging to clippings of the same image (cf. the curves in the second row of Figure 5 and 6). There, however, was a relation between the noise variance curve and the histogram of the individual clipping (cf. Figure 3, rows 1 to 3, and Figure 5 and 6, rows 1 and 2).

Large differences between the intensities of corresponding pixels in the successive images of one scan series lead to high values for the noise standard deviation. Looking at the differences between the images of a scan series (Figure 2), we can

see that the largest differences can be found at sharp edges, where the gradient is steep.

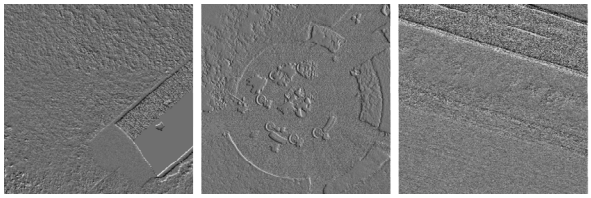

Figure 2: Intensity differences between the 1st and the 10th scan of the scan series for image clipping B, A3 and A'. Grey = 0 [gv], dark = negative difference, light = positive difference

This means that the resulting noise variance function depends on the presence of edges in the analyzed image clipping. The noise standard deviations in the diagrams in the second and third row of Figure 3 show the combined effect of edge pixels and pixels with lower noise variance.

In order to separate the two categories, we set a threshold to exclude pixels with high gradients, and compute again the noise variance. The behaviour of the noise standard deviation after the exclusion of the influence of pixels with high gradients is plotted in the fourth row of Figure 3. The first two curves, belonging to the clippings B and A3, show a smooth behaviour. The small peaks can at least partly be explained by the inclusion of pixels close to edges. For the other clippings of image A we obtain the same curve (cf. Figure 5, diagrams in row 3), while for A' the curve lies slightly lower.

The curve for clipping D2 shows a non-linear behaviour. The same course can be found for all the clippings of image D (cf. diagrams in the last row of Figure 6). As image D is the only colour test image and the information we had about the film material was feeble, it is premature to hazard hypothesis.

An explanation for the scattering of the σ_n of contiguous intensity values can be found when looking at the histogram of the clipping (first row of Figure 3). It is found that they correspond to intensity classes including only a small number of values, which of course lead to large scatter of the estimated variances.

The distribution of the intensities at the same pixel in the different images of a scan series can be analyzed by means of the MAD^+ and the MAD^-. When looking at the fifth row of diagrams in Figure 3, showing the median of $\sigma_{n,med+}$ and $\sigma_{n,med-}$ for classes of 8 [gv] width, we can see that the distribution is not symmetric about the median of the intensities. The $\sigma_{n,med-}$ shows a regular behaviour, the values increasing towards high intensities, while the curve of the $\sigma_{n,med+}$ is irregular. This behaviour is common to all the analyzed images.

4.3 Correlations between multiple scans

The correlation function $\rho_{g'g''}$ was computed for all combinations within the 10 scans of image C'.

First the SNR was calculated from equation (13). The results are listed in Table 2. The SNR values over the image series cover a range from 37.6 to 25.6.

The signal variance σ_g for the test image amounts ≈ 23 [gv]. We calculate the noise σ_n by means of the SNR, obtaining for σ_n a range from 0.6 [gv] to 0.9 [gv]. The corresponding curve obtained analyzing the noise variance pixelwise for the multiple scans of image C, from which C' was cropped, shows a σ_n of 0.4 [gv] to 0.5 [gv]. The noise standard deviation obtained by means of the image correlation is about a factor 1.4 higher, which, though a significant difference, resulting from the effect of the edge pixels, confirms the estimates to be reliable.

When looking at the differences between successive scans, a trend becomes clearly visible, which also confirms the results of Table 2. As can be seen on the bases of Table 3 and in Figure 4, the differences for immediately successive scans of an image remains almost constant, while it increases if considering later images of the same scan series.

	1	2	3	4	5	6	7	8	9	10
1	—									
2	34.0	—								
3	36.0	34.3	—							
4	34.0	33.9	37.1	—						
5	32.8	32.8	36.6	37.4	—					
6	31.2	31.4	35.3	36.0	36.9	—				
7	29.6	30.6	34.0	35.4	36.5	37.5	—			
8	28.4	29.8	32.8	34.5	35.9	36.5	37.6	—		
9	27.6	29.3	31.8	33.6	35.1	36.0	37.0	37.6	—	
10	25.6	27.1	29.2	31.1	31.7	32.3	34.2	34.5	34.3	—

Table 2: $SNR = \sqrt{\rho/(1-\rho)}$ for the possible combinations of scans of an image series for clipping C', calculated by means of the correlation coefficient ρ

1. scan	2. scan	min [gv]	max[gv]	1.image	2.image	min[gv]	max[gv]
1	2	-18	20	1	2	-18	20
2	3	-11	11	1	3	-21	23
3	4	-12	13	1	4	-30	29
4	5	-11	12	1	5	-33	32
5	6	-12	12	1	6	-38	36
6	7	-11	12	1	7	-45	42
7	8	-12	12	1	8	-41	43
8	9	-12	11	1	9	-44	46
9	10	-12	11	1	10	-48	50

Table 3: Range of intensity differences between different scans of the series for clipping A3. On the left the differences between successive scans, on the right the differences between the first scan and the other scans.

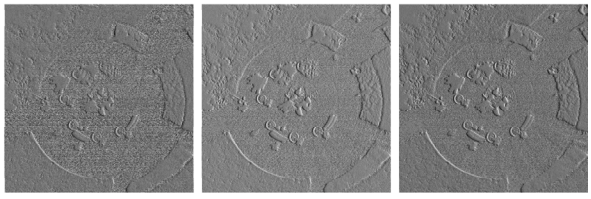

Figure 4: Intensity differences between the 1st and the 2nd, the 1st and the 5th and the 1st and the 10th scan of the scan series for image clipping A3

For images with more homogeneous contents the difference range is smaller, but the same trend can still be observed. In each of the analyzed image series the differences between the first and the second scanned images were larger than between every other pair of images scanned one after the other.

The determination of the location of the point of maximal correlation with sub-pixel accuracy allows us to determine the geometric displacement between different digitizations in

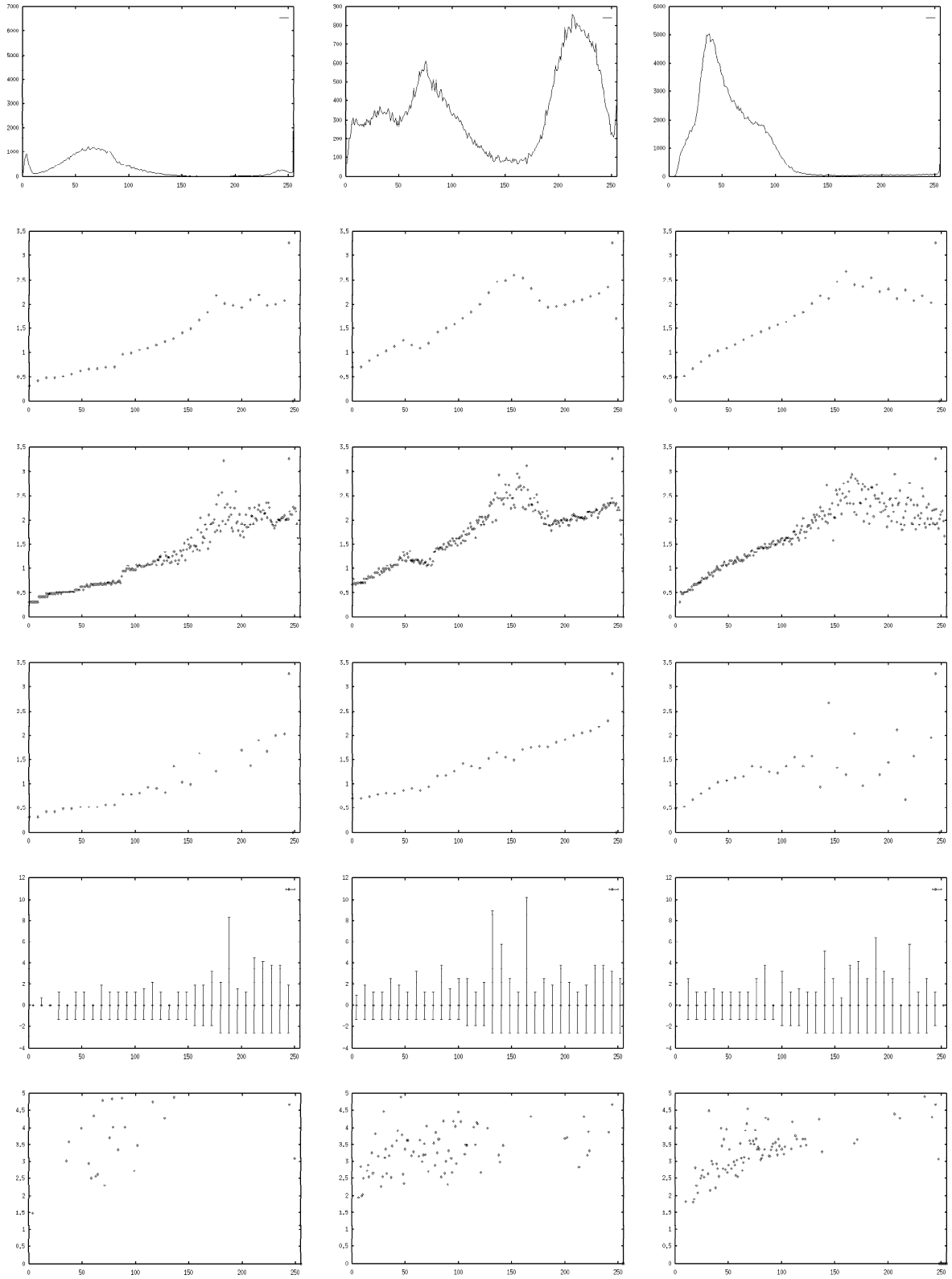

Figure 3: Columnwise the noise standard deviation σ_n as a function of the intensity g are plotted for clipping B (left), A3 (middle) and D2 (right).

1st row: histogram of the clipping

2nd row: $\sigma_{n,mean}$ [gv] from pixelwise analyse of multiple scans, for classes of 8 [gv]

3rd row: $\sigma_{n,mean}$ [gv] from pixelwise analyse of multiple scans, for classes of 1 [gv]

4th row: same as 2nd row, after the exclusion of pixels with a high gradient

5th row: $\sigma_{n,med+}$ [v] and $\sigma_{n,med-}$ [gv] for classes of 8 [gv]

6th row: $\sigma_{n,mean}$ [gv] from homogeneous regions of a single scan

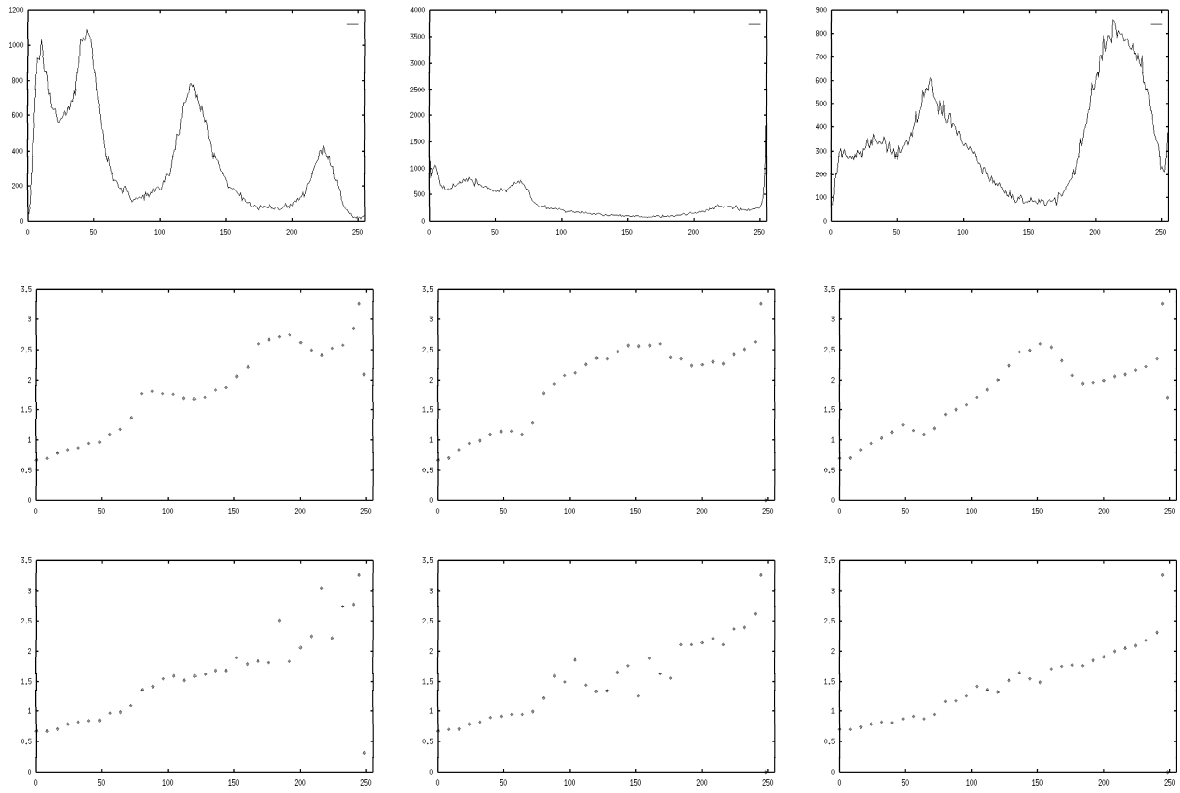

Figure 5: Histogram (row 1) and noise standard deviation $\sigma_{n,mean}$ [gv] as a function of the intensity g for classes of 8 [gv] before (row 2) and after (row 3) the exclusion of the edge pixels from the noise variance estimation, for the clippings A1, A2 and A3 of the same image

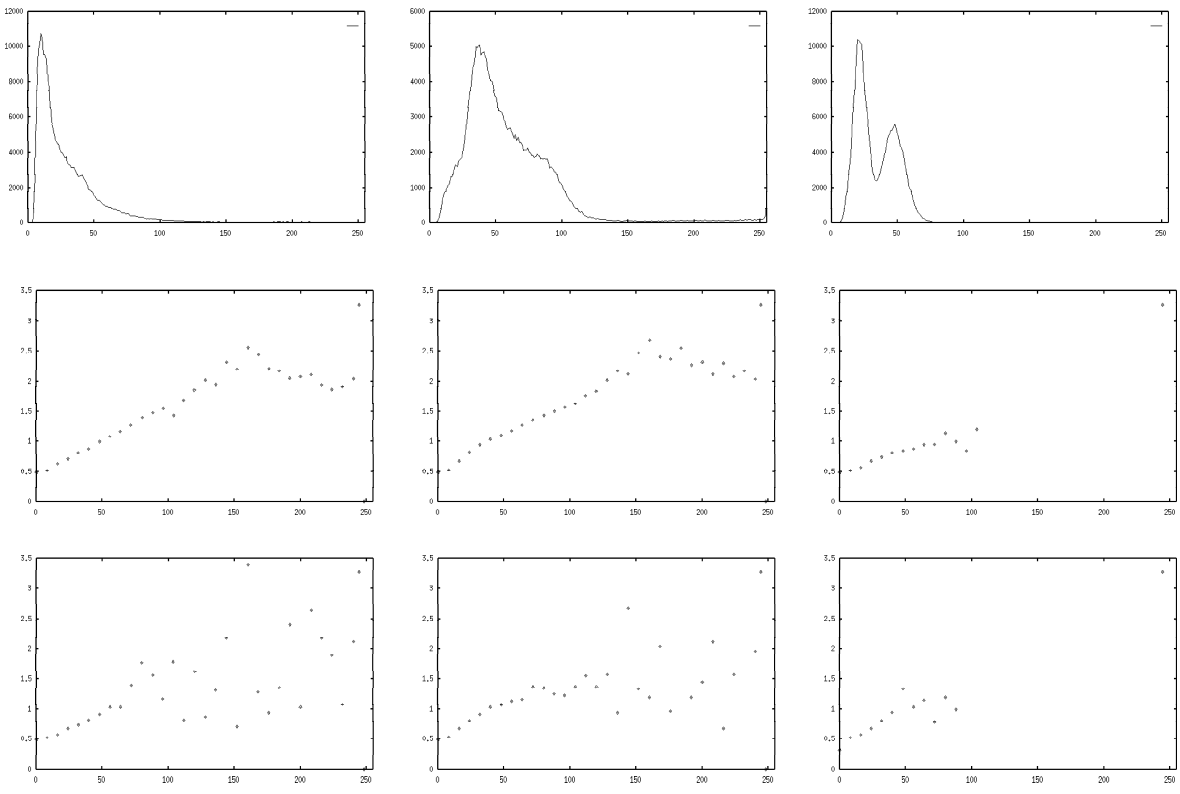

Figure 6: Histogram (row 1) and noise standard deviation $\sigma_{n,mean}$ [gv] as a function of the intensity g for classes of 8 [gv] before (row 2) and after (row 3) the exclusion of the edge pixels from the noise variance estimation, for the clippings D1, D2 and D3 of the same image

a scan series. The displacement is mainly due to the mechanical positioning accuracy. Another component is of electronic nature and arises from the A/D conversion.

We calculated the displacements between the first and the last scan of every clipping series. The displacements cover a range from 0.04 μm up to 2.5 μm in the sensor direction and from 0.1 μm to 2.2 μm in the scan direction, yielding a total displacement of up to 3.3 μm. All the displacements in scan direction are positive. When comparing the displacements for clippings of the same scan series, only for the displacement in sensor direction of image A (corresponding to the clippings A1, A2 and A3) the hypothesis of a systematic displacement is admissible. To be able to make reliable statements, a larger sample of scans should be analyzed.

	A1	A2	A3	A'	B	C	C'	D1	D2	D3
Δx [μm]	-2.4	-2.5	-2.5	-0.4	-0.04	0.04	0.6	-1.2	0.2	0.7
Δy [μm]	2.2	0.9	0.5	0.7	1.9	0.2	0.1	1.5	1.2	0.5
$\lvert\Delta_{tot}\rvert$ [μm]	3.3	2.8	2.5	0.8	1.9	0.2	0.6	1.9	1.2	0.9

Table 4: Displacements between the first and the last image of a scan series, for all test clippings

4.4 Noise variance from single scans

The minimum size for the extracted regions to be considered was set to 9 pixels, while no upper limit was set. The size of the extracted regions was not used as a weighting criterion, because it gives no warranty about the absence of residual texture.

The last row of diagrams in Figure 3 shows the noise standard deviation for the detected homogeneous regions. The basic noise variance is higher than the one observed in the analysis of multiple scans, which is due to the additional noise components. In dependence of the features present in the analyzed clipping, it can be impossible to predict a noise variance function for the whole intensity range (as the diagram for clipping B shows). The diagrams for clipping A3 and D2 show a basic noise [gv] and a band structure where the form of the function determined in the analysis of the multiple scans can be found again. The same structure can also be found in the corresponding plots for the other clippings of the same image, and the width of the band structure is constant within one scan series.

The regions detected by the feature extraction algorithm are not guaranteed to be homogeneous enough to permit a reliable estimation of the image noise. The estimated noise variance therefore often is much larger than the pure scanning noise, and probably contains effects of smooth intensity variations, moderate texture or other small irregularities. An improved estimate from single scans would be obtained if only the local gradients are used.

5 CONCLUSIONS AND OUTLOOK

The scope of this paper was to determine a noise model out of digitized images without the need for special test patterns. We followed two approaches: a pixelwise evaluation of multiple scans of the film material and a regionwise evaluation from single scans. The first approach analyses the noise coming from the digitization process alone, while in the second case we find the complete noise budget.

We found the following results:

- The noise standard deviation in the analysed images ranges from 0.5 to 3 [gv], which confirms the high performance of the scanner.
- In all cases the noise variance significantly increases with the intensity.
- The pixelwise analysis of multiple scans using all pixels yields an irregular noise variance curve $\sigma_n(g)$. It depends on the image clipping used for the analysis. Different clippings of the same image show different estimated noise variance curves.
- The pixelwise analysis of multiple scans excluding edge pixels yields a smooth noise variance curve. It shows consistency between different clippings of the same image.
- The geometric stability of the scanner limits the noise analysis with repetitive scanning, especially in case of pixel sizes below 30 μm.
- The geometric stability is within 3 μm maximum shift between successive scans.
- The performed analysis of single scans, yielding the total noise variance, showed significantly larger noise. This certainly is due to the nonconstancy of the intensity within the regions. Deriving the noise variance from local intensity differences would reduce this effect.

We are aiming at a characterization of the noise of digitized aerial images depending on pixel size and scan parameters. We are also investigating the temporal behaviour of the scanner noise variance. It is planned to consider separately the behaviour of the intensities in scan and in sensor direction, to take into account the different scan principles in the two directions. All these investigations need to be performed for other high precision film scanners resulting in practical guidelines for image analysis tools. We intend to investigate the effect of the image noise onto basic photogrammetric mensuration operations, especially onto extraction of points and edges and onto image matching.

REFERENCES

[Baltsavias et al., 1997] Baltsavias, E. P., Häring, S., and Kersten, T. (1997). Geometric and Radiometric Performance Evaluation of the Leica/Helava DSW200 Photogrammetric Film Scanner. *SPIE*, 3174:157–173.

[Baltsavias and Käser, 1998] Baltsavias, E. P. and Käser, C. (1998). Evaluation and Testing of the Zeiss SCAI Roll Film Scanner. *Proceedings of ISPRS Commission I Symposium, Bangalore, India. In International Archives of Photogrammetry and Remote Sensing*, 32/1.

[Bolte et al., 1996] Bolte, U., Jacobsen, K., and Wehrmann, H. (1996). Geometric and Radiometric Analysis of a Photogrammetric Image Scanner. *Proceedings of the 18th ISPRS Congress, Vienna, Austria. In International Archives of Photogrammetry and Remote Sensing*, 31(B1):72–77.

[Brügelmann and Förstner, 1992] Brügelmann, R. and Förstner, W. (1992). Noise Estimation for Color Edge Extraction. In Förstner, W. and Ruwiedel, S., editors, *Robust Computer Vision*, pages 90–107. Wichmann, Karlsruhe.

[Dainty and Shaw, 1974] Dainty, J. C. and Shaw, R. (1974). *Image Science*. Academic Press.

[Diehl, 1990] Diehl, H. (1990). Radiometric Noise in Digitized Photographs. In *SPIE Vol. 1395, Close-Range Photogrammetry Meets Machine Vision*, pages 90–106. Wichmann Verlag Bonn.

[Diehl, 1992] Diehl, H. (1992). Optimal Digitization Steps for Usual Film Materials. *Proceedings of the 17th ISPRS Congress in Washington. International Archives of Photogrammetry and Remote Sensing*, 29/B1:1–6.

[Häring et al., 1998] Häring, S., Kersten, T., Dam, A., and Baltsavias, E. P. (1998). Quality Analysis of the LH Systems DSW300 Roll Film Scanner. *Proceedings of ISPRS Commission I Symposium, Bangalore, India. In International Archives of Photogrammetry and Remote Sensing*, 32/1.

[Lenz, 1988] Lenz, R. (1988). Zur Genauigkeit der Videometrie mit CCD-Sensoren. In *Mustererkennung 1988 (DAGM-Symposium)*, pages 179–189.

[Roth, 1996] Roth, G. (1996). Quality Features of a State-of-the-Art High-Performance Photogrammetric Scanning System: PHODIS SC. *Proceedings of the 18th ISPRS Congress, Vienna, Austria. In International Archives of Photogrammetry and Remote Sensing*, 31(B1):163–166.